Electronic Supplementary Material (ESI) for Physical Chemistry Chemical Physics.


# Electronic Supplementary Information

## Mesoporous $Li_4Ti_5O_{12-x}$/C submicrospheres with comprehensively improved electrochemical performances for high-power lithium-ion batteries

Chunfu Lin[a], Man On Lai[a], Henghui Zhou[b]*, Li Lu[a]*

[a] *Department of Mechanical Engineering, National University of Singapore, 9 Engineering Drive 1, Singapore 117576, Singapore*

[b] *College of Chemistry and Molecular Engineering, Peking University, Beijing 100871, PR China.*

* *Corresponding authors. Tel.: +65 65162236; fax: +65 67791459. E-mail address: luli@nus.edu.sg (L. Lu).*

*Tel.: +86 10 62757908; fax: +86 10 62757908. E-mail address: hhzhou@pku.edu.cn (H. Zhou).*

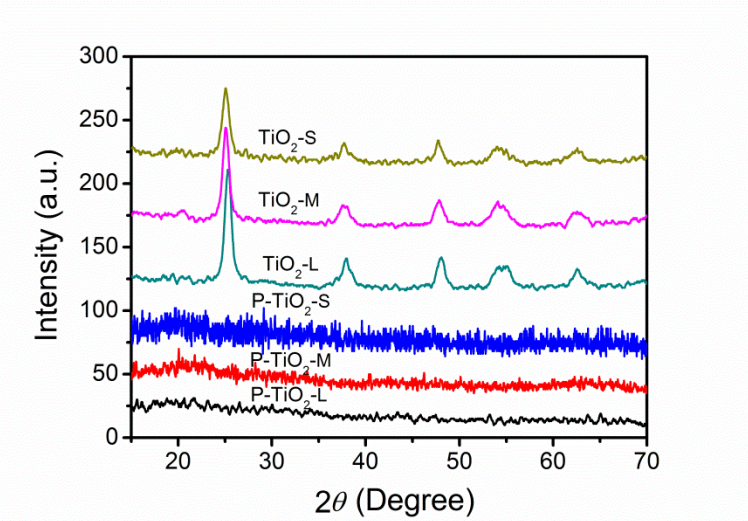


Fig. S1. XRD spectra of P-$TiO_2$-L, P-$TiO_2$-M, P-$TiO_2$-S, $TiO_2$-L, $TiO_2$-M and $TiO_2$-S.

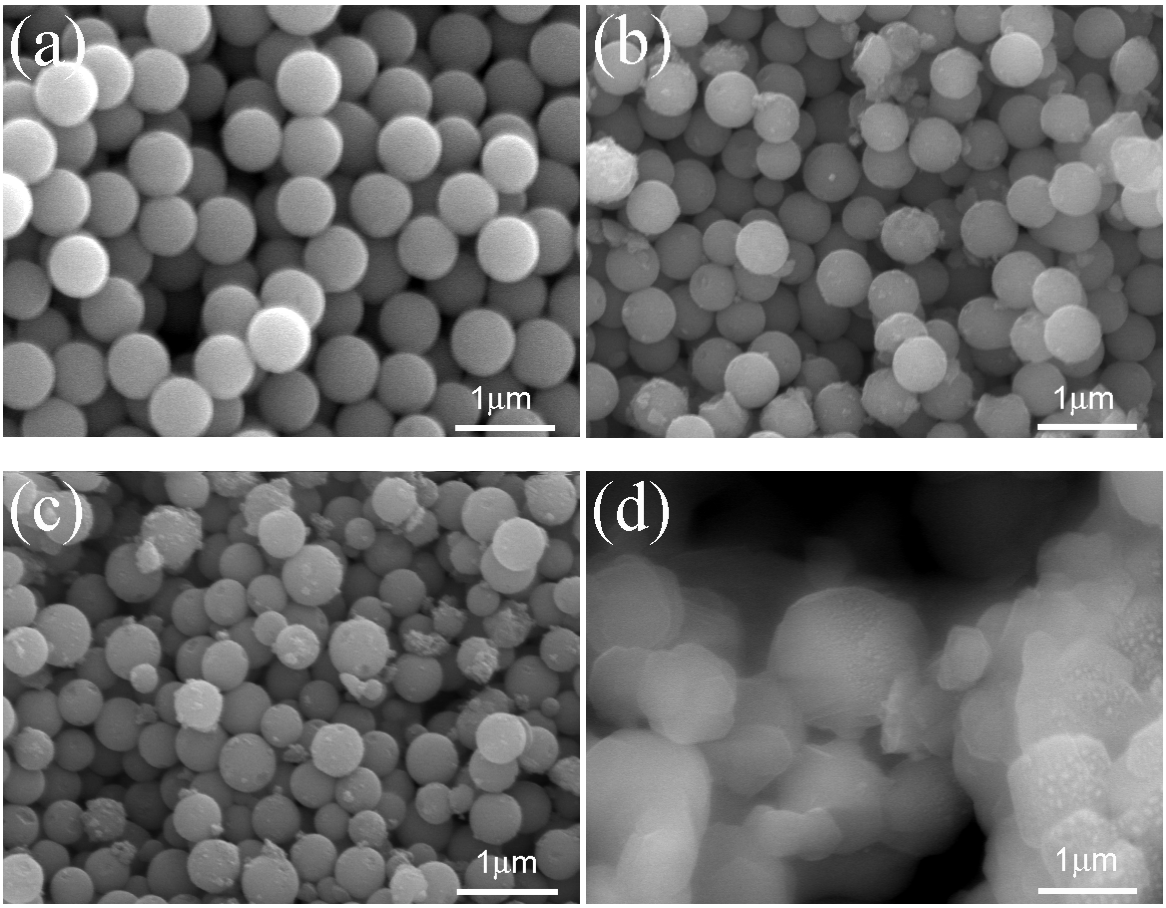


Fig. S2. FESEM images of (a) $TiO_2$-L, (b) $TiO_2$-M, (c) $TiO_2$-S and (d) LTO-S.

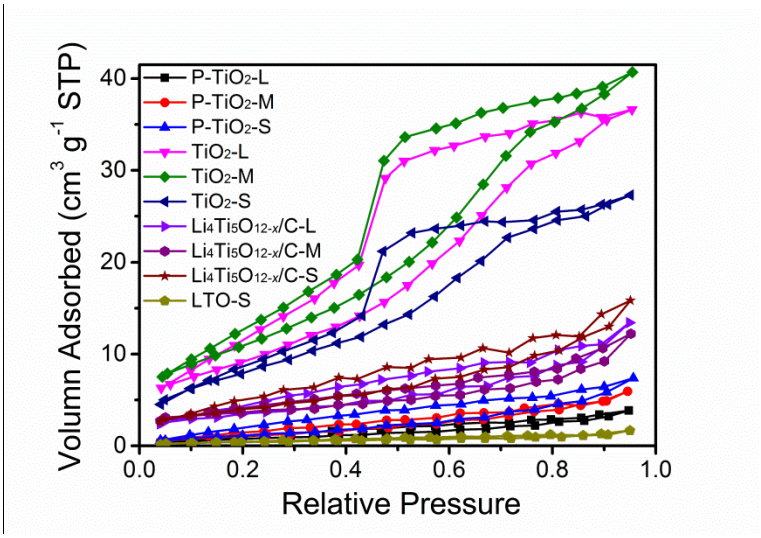


Fig. S3. Nitrogen adsorption–desorption isotherms of P-$TiO_2$-L, P-$TiO_2$-M, P-$TiO_2$-S, $TiO_2$-L, $TiO_2$-M, $TiO_2$-S, $Li_4Ti_5O_{12-x}$/C-L, $Li_4Ti_5O_{12-x}$/C-M, $Li_4Ti_5O_{12-x}$/C-S and LTO-S.

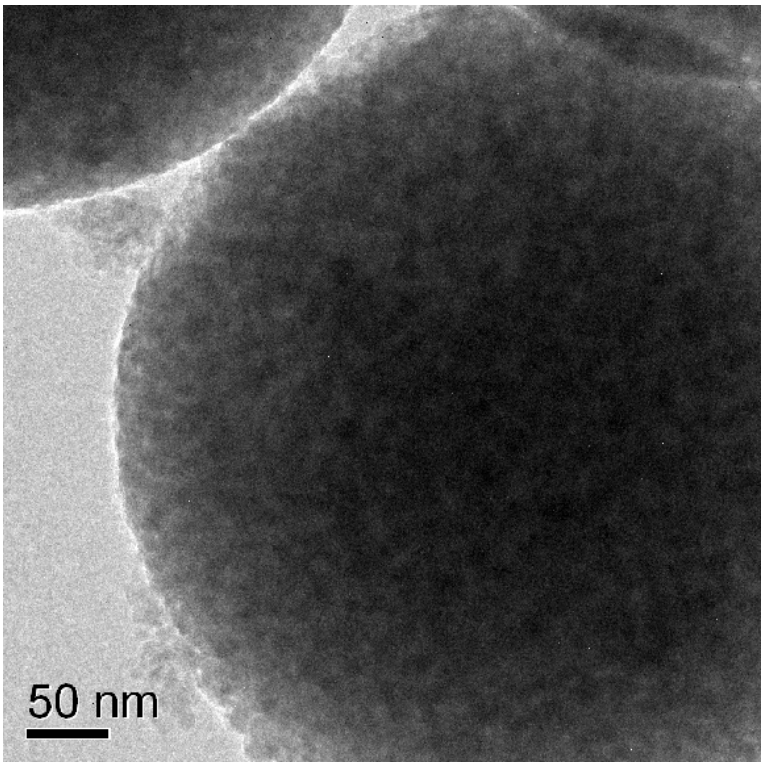


Fig. S4. TEM image of $TiO_2$-L.

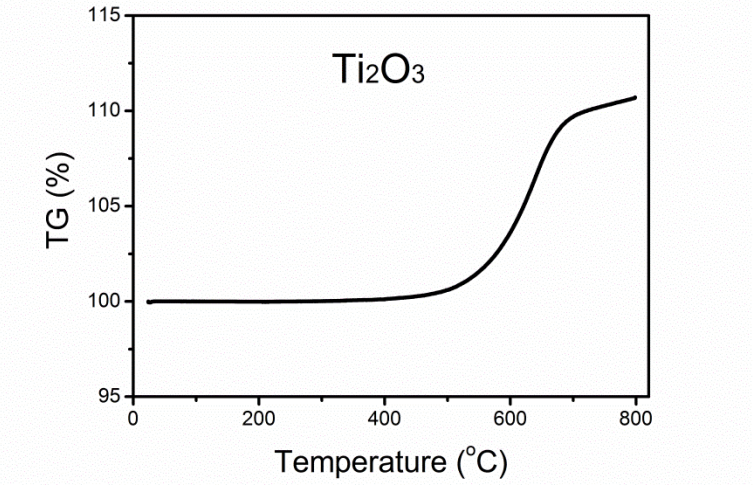


Fig. S5. TG curve of $Ti_2O_3$ powders.

**Refinement process:**

Three constraints for the refinements have been set. Firstly, the site occupancies of the LTO-type crystals in the three composites fulfill stoichiometric composition of $Li_4Ti_5O_{12-x}$, while that of LTO-S follows

$Li_4Ti_5O_{12}$. Secondly, the contents of $Ti^{3+}$ and $Ti^{4+}$ ions are fixed based on the TG results. Finally, the distribution of ions in the spinel structure is fixed as follows: $O^{2-}$ ions were located at 32e sites; $Li^{+}$ and $Ti^{4+}$ ions are distributed at both 16d and 8a sites while $Ti^{3+}$ ions only stay at 16d sites. In principle, $Ti^{3+}$ ions can reside at both 16d and 8a sites. However, it is impossible by the refinements of the X-ray diffraction profiles to distinguish $Ti^{3+}$ and $Ti^{4+}$ ions because these two kinds of ions have very close X-ray scattering factors. $Ti^{3+}$ ion has a octahedral site preference energy (OSPE, 28.89 kJ $mol^{-1}$) significantly larger than $Ti^{4+}$ ion (0 kJ $mol^{-1}$) [S1], inferring that $Ti^{3+}$ ion has a tendency to occupy 16d sites much higher than $Ti^{4+}$ ion. Therefore, to proceed the refinements, it can reasonably be assumed that $Ti^{3+}$ ions only stay at 16d sites, while $Ti^{4+}$ ions are distributed in both 16d and 8a sites. In the refinement process, background parameters, zero-shift, unit cell parameters, profile parameters, atomic fractional coordinates, atomic isotropic displacement parameters and atomic occupancies were successively refined.

**Reference**

[S1] R. G. Burns, Mineralogical Applications of Crystal Field Theory, Cambridge University Press, Cambridge, 2nd edn, 1993.

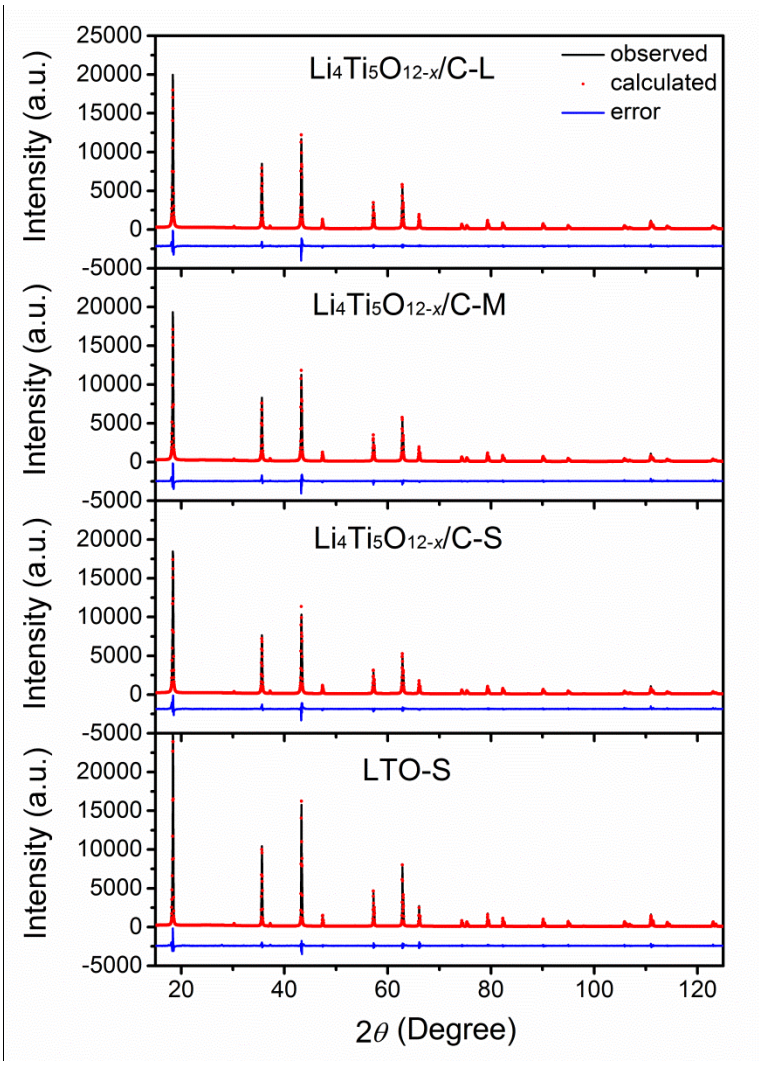


Fig. S6. Rietveld refinement patterns for $Li_4Ti_5O_{12-x}$/C-L, $Li_4Ti_5O_{12-x}$/C-M, $Li_4Ti_5O_{12-x}$/C-S and LTO-S.

Table S1. Material characteristics of prepared powders.

| Sample | Sphere size (nm) | Primary particle size (nm) | Crystallinity | Specific surface area ($m^2$ $g^{-1}$) | Pore size (nm) | Pore volume ($cm^3$ $g^{-1}$) | Carbon content (%) | Tap density (g $cm^{-3}$) |
|---|---|---|---|---|---|---|---|---|
| P-$TiO_2$-L | 800±30 | – | amorphous | 3.35 | 4.42 | 0.006 | – | – |
| P-$TiO_2$-M | – | – | amorphous | 4.51 | 4.92 | 0.009 | – | – |
| P-$TiO_2$-S | – | – | amorphous | 4.99 | 5.42 | 0.011 | – | – |
| $TiO_2$-L | 610±30 | ~10 | poor | 35.5 | 4.04 | 0.057 | – | – |
| $TiO_2$-M | – | ~10 | poor | 41.3 | 3.90 | 0.063 | – | – |
| $TiO_2$-S | – | ~10 | poor | 31.0 | 3.57 | 0.042 | – | – |
| $Li_4Ti_5O_{12-x}$/C-L | 530±30 | mainly <100 | high | 12.3 | 3.92 | 0.019 | 1.44 | 1.41 |
| $Li_4Ti_5O_{12-x}$/C-M | – | mainly <100 | high | 12.2 | 4.26 | 0.021 | 1.28 | 1.57 |
| $Li_4Ti_5O_{12-x}$/C-S | – | mainly <100 | high | 14.6 | 4.19 | 0.025 | 1.06 | 1.71 |
| LTO-S | – | 200–3000 | high | 1.52 | 3.40 | 0.002 | – | 1.22 |

Table S2. Electrochemical performances of $Li_4Ti_5O_{12-x}$/C-L, $Li_4Ti_5O_{12-x}$/C-M, $Li_4Ti_5O_{12-x}$/C-S and LTO-S samples.

| Sample | Discharge potential at 0.1 C (mV) | Charge potential at 0.1 C (mV) | Working potential at 0.1 C (mV) | Charge capacity at 0.5 C (mAh $g^{-1}$) | Charge capacity at 1 C (mAh $g^{-1}$) | Charge capacity at 2 C (mAh $g^{-1}$) | Charge capacity at 5 C (mAh $g^{-1}$) | Charge capacity at 10 C (mAh $g^{-1}$) | First cycle Coulombic efficiency (%) | Capacity retention over 100 cycles (%) | $R_\Omega$ (Ω) | $R_s$ (Ω) | $R_{ct}$ (Ω) |
|---|---|---|---|---|---|---|---|---|---|---|---|---|---|
| $Li_4Ti_5O_{12-x}$/C-L | 1552.8 | 1569.0 | 1560.9 | 160 | 152 | 144 | 129 | 108 | 94.6 | 95.8 | 2.08 | 313 | 734 |
| $Li_4Ti_5O_{12-x}$/C-M | 1553.9 | 1567.3 | 1560.6 | 162 | 156 | 149 | 133 | 113 | 93.8 | 95.5 | 2.62 | 296 | 635 |
| $Li_4Ti_5O_{12-x}$/C-S | 1554.7 | 1566.8 | 1560.8 | 163 | 159 | 153 | 138 | 118 | 95.0 | 95.9 | 2.48 | 274 | 474 |
| LTO-S | 1556.2 | 1574.4 | 1565.3 | 148 | 115 | 72 | 27 | 12 | 96.1 | – | 3.59 | – | 1021 |